X線分析の進歩 第40集（2009）抜刷
Advances in X-Ray Chemical Analysis, Japan, 40 (2009)
アグネ技術センター
ISSN 0911-7806

X-Ray Analysis of Yb Ultra Thin Film: Comparison of Gas Deposition and Ordinary Vacuum Evaporation

Martin JERAB and Kenji SAKURAI

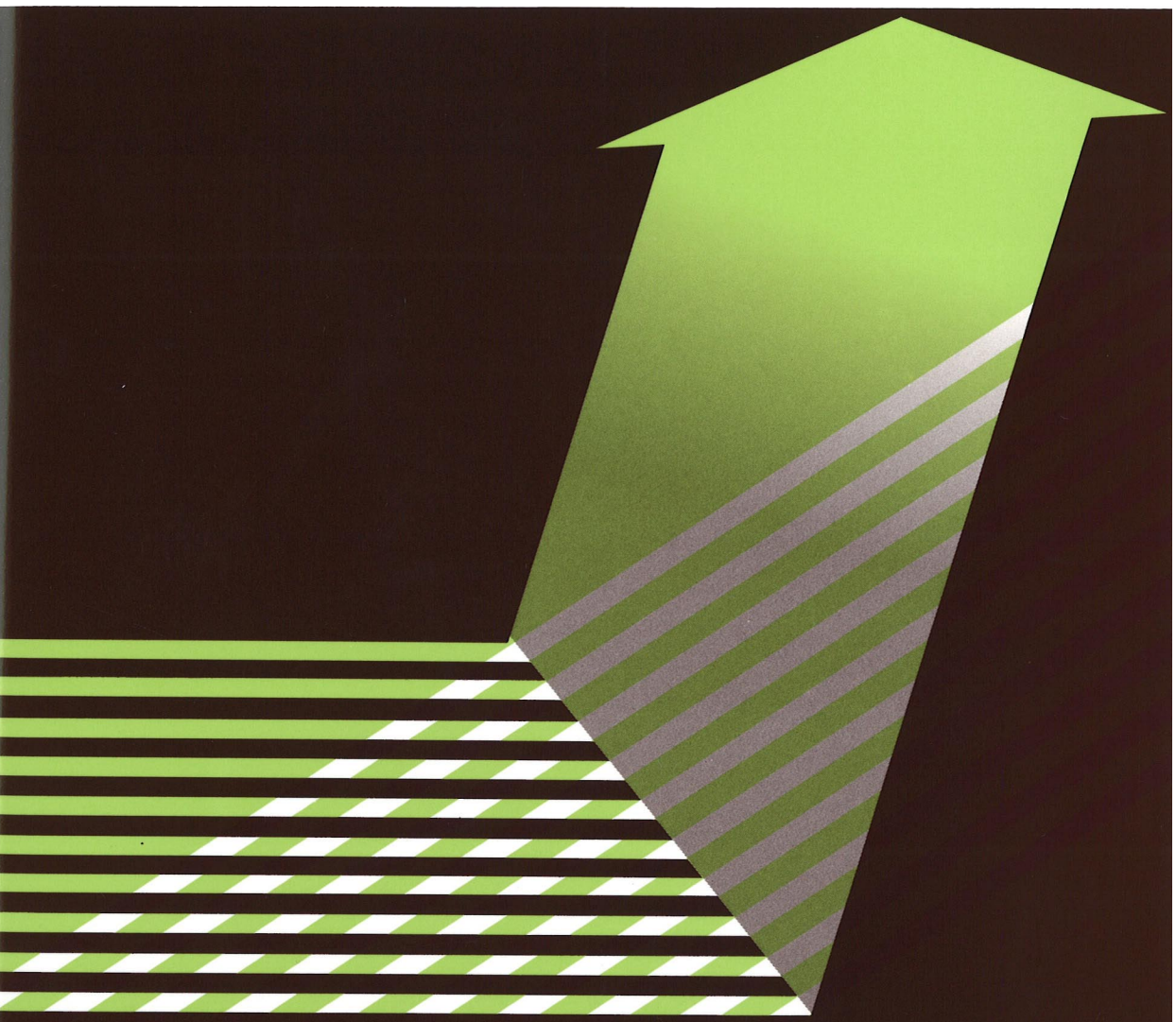

X-Ray Analysis of Yb Ultra Thin Film: Comparison of Gas Deposition and Ordinary Vacuum Evaporation

Martin JERAB* and Kenji SAKURAI#

National Institute for Materials Science
1-2-1 Sengen, Tsukuba, Ibaraki 305-0051, Japan
* Charles University, Faculty of Mathematics and Physics
V Holesovickach 2, Praha 8, 180 00, Czech Republic
Corresponding author: sakurai@yuhgiri-nims.go.jp

(Received 7 January 2009, Revised 16 January 2009, Accepted 19 January 2009)

Nanotechnology has gained big importance in the last decade in the areas of basic research and applied science. One part of nanotechnology is preparation of nanoparticles where new, not ordinary, materials are recently used. In the present study, we succeeded in the preparation of ytterbium nanoparticles by employing the gas deposition method preparing particles with a variety of sizes. We combined several different techniques to perform investigations of the properties of films from nanoparticles such as the thickness of deposited film, interface parameters, the size distribution of nanoparticles, their crystal structure, etc. and their dependence on deposition parameters.
[Key words] Nanoparticles, Ytterbium, Gas deposition, Thin film, AFM, XRR, XRD

1. Introduction

Preparation of nanoparticles has become an important issue not only in basic research but also in applied nanotechnology. In particular, nanoparticles from rare earth elements are attractive due to their specific chemical and physical properties. One of the most interesting elements in the lanthanide series is ytterbium (Yb) [1], often serves as a dopant for a variety of functional materials. Due to its unique electrical properties, it is usually used in active media for optics (YAG laser). So far, there have been very limited reports on the formation of Yb particles because their successful synthesis by chemical routes was achieved only a few years ago [2]. In the present study, we have employed a completely different technique, the gas deposition method [3].

The technique is based on the vacuum deposition method. Metallic ytterbium is evaporated by heating in a gas atmosphere (in our case He). The particles are formed by solidification and aggregation during collisions with the gas molecules. The particles lose almost all their thermal kinetic energy during the collision. Based on this, the landing of the nanoparticles on the substrate is very soft and the nanoparticles do not deposit any energy on the substrate. A similar method was successfully applied to produce gadolinium nanoparticles [4].

独立行政法人 物質・材料研究機構　茨城県つくば市千現 1-2-1　〒 305-0047　　# 連絡著者：sakurai@yuhgiri-nims.go.jp
＊チェコ共和国 チャールス大学 数学物理学部　V Holesovickach 2, Praha 8, 180 00, Czech Republic

2. Experimental setup

The apparatus used in the present gas deposition experiment is basically a vacuum evaporation chamber (10^{-6} Pa) equipped with a Knudsen evaporation cell (K-cell) and sample load lock system [4]. The experiments can be switched from the ordinary vacuum evaporation to gas deposition simply by introducing the He gas. An illustrative scheme of the entire apparatus and components of the main chamber (MCh) is shown in Fig.1. The apparatus is composed of two chambers (main chamber MCh, load lock chamber LLCh) which are separately pumped by turbo molecular pumps. The load lock chamber with linear motion of samples is separated from the main chamber by a gate valve. This set-up allows us to perform preparation of nanoparticles in clean and well controlled conditions and prevents contamination during deposition. The pressure in the chamber before injection of the gas was about 10^{-6} - 10^{-7} Pa (10^{-8} -10^{-9} Torr). On the bottom of the main chamber there was a K-cell with shutter. Metallic ytterbium was evaporated by heating (500 ~ 825°C, melting point is 824°C) in the He environment (0.5~25 Pa). The evaporating temperature was controlled by a heating control unit with an accuracy of 0.5 °C. The particles were formed by solidification and aggregation during the collisions with inert He gas molecules. To collect floating particles, the glass substrate was placed close (10 mm) to the top of the K-cell. In order to eliminate

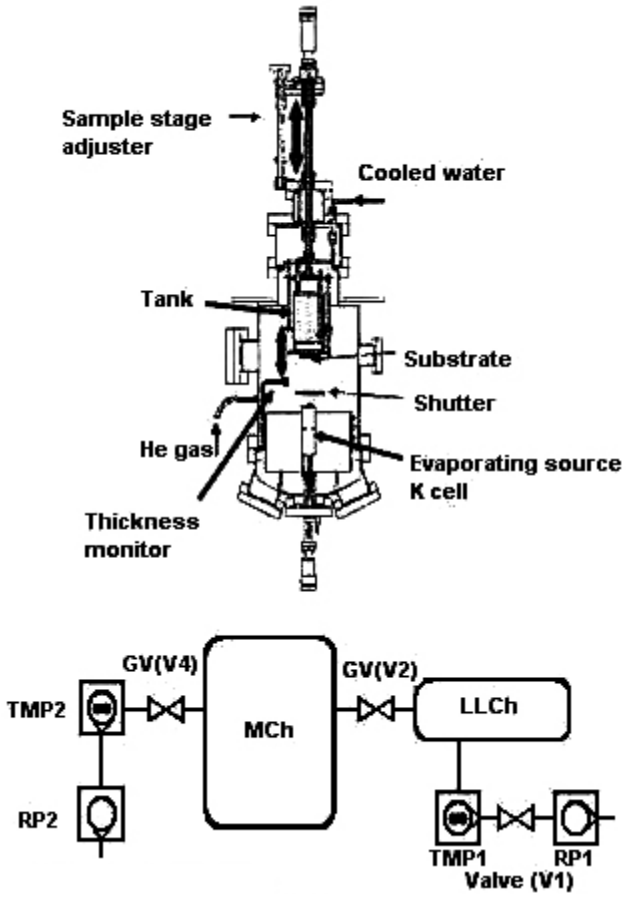

Fig.1 Figure shows illustrative schemes of the gas deposition apparatus. The apparatus is basically a vacuum evaporation chamber (10^{-6} Pa) equipped with a Knudsen evaporation cell (K-cell) and sample load lock system [4]. The experiments can be switched from the ordinary vacuum evaporation to gas deposition simply by introducing the He gas. MCH: Main chamber, LLCh: Load lock chamber, RP: Rotary pump, TMP: Turbo molecular pump, GV: Gate valve

further aggregation of nanoparticles at the substrate surface by radiation heating, the back of the substrate was cooled. The deposition rate is measured by a quartz thickness monitor.

3. Measurement technique

The deposited thin film composed of nanoparticles was analyzed using several different techniques. The size distribution of the deposited nanoparticles was analyzed by processing atomic force microscope (AFM) images (Shimadzu SPH-9500J3). Surface roughness was also examined by this method and compared with the results of X-ray reflectivity measurements (XRR). In addition, this technique was used to determine the thickness of the deposited film, as well as to estimate surface and interface roughness. The MUREX software [5] was used for XRR data processing as follows. Theoretical simulation of XRR was computed with Parratt's formalism [6] using a layer model at the top of the glass substrate. Simulated curve was compared with experimental data and the model's parameters (thickness, density, surface/interface roughness, scaling factor) were manually changed to optimize the fitting of both curves. Goodness of fit was evaluated by the same software by $|R_{exp}(i) - R_{calc}(i)|^2$ least-squares method and determined from the

$$R_p \left(= \frac{\sum \left| R_{exp}(i) - R_{calc}(i) \right|}{\sum R_{exp}(i)} \right)$$

and

$$R_{wp} \left(= \sqrt{\frac{\sum \left(R_{exp}(i) - R_{calc}(i) \right)^2}{\sum R_{exp}(i)^2}} \right)$$

factor in log scale. An R-factor less than 4% was an acceptable fit. The computer fitting was then performed with the initial parameters taken from "manual" fitting to optimize the parameters, determine the best-fit values and further reduce the R-factor. The best-fit values were taken to be the thickness, density and surface/interface roughness for the nanoparticles thin film. The crystal structure of the deposited nanoparticles was studied by X-ray diffraction (XRD) and grazing incidence in the plane X-ray diffraction (IPXRD). Rigaku PINT-ATX was used for all X-ray measurements.

4. Results and Discussion

While ordinary vacuum evaporation produces islands, i.e., particles stacked together (Fig.2), the technique used in the present study (gas deposition) allows us to obtain nanoparticles. From the AFM measurement, it was found that the particles have an almost spherical shape with quite a small variation in size for each sample (Figs.3, 4). The size is typically around 4 nm in diameter. This indicates that one

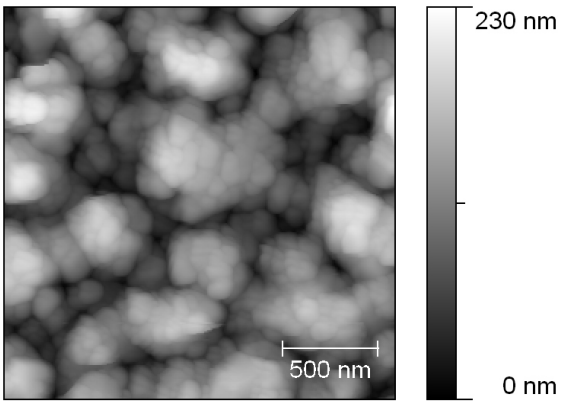

Fig.2 AFM image of sample prepared by vacuum deposition under following condition; deposition temperature t_d = 600 °C, deposition pressure P = 3.8×10^{-6} Pa, deposition time t = 3 hours. The figure shows that the deposit is composed of islands, i.e., particles stacked together.

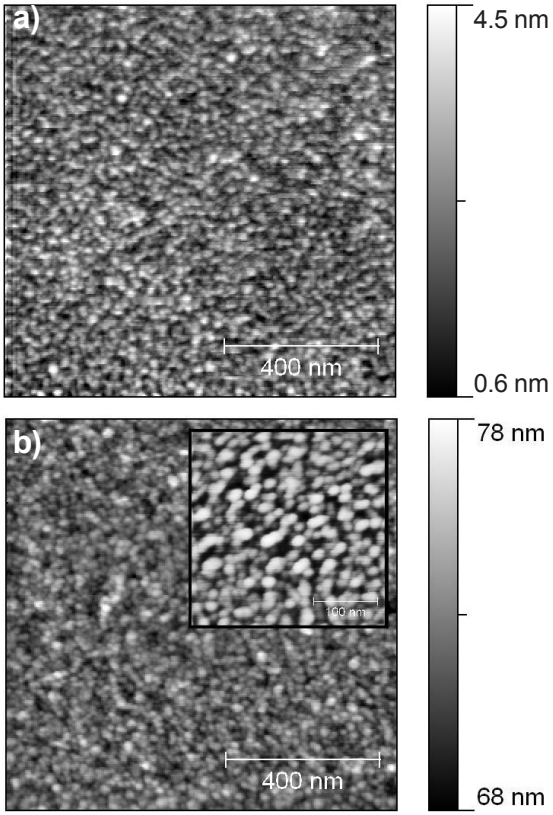

Fig.3 AFM images of samples prepared under following conditions; a) deposition temperature t_d = 700 °C, deposition pressure P = 3 Pa, deposition time t = 3 hours, b) t_d = 825 °C, deposition pressure P =3 Pa, deposition time t = 3 hours. The nanoparticles for both samples are spherical. The mean size of the nanoparticles is d = 1.6 ± 1.2 nm, d = 2.5 ± 1.8 nm respectively [7].

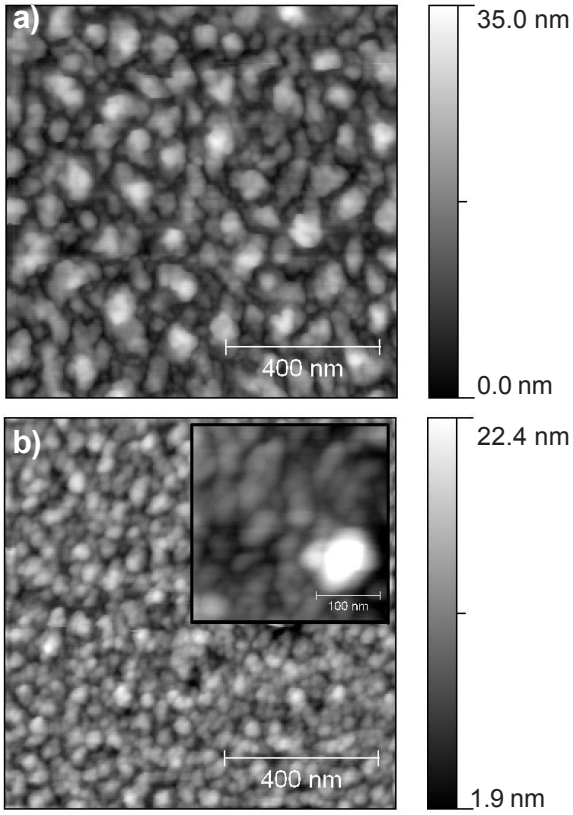

Fig.4 AFM images of samples prepared under following conditions; a) deposition temperature t_d = 500 °C, deposition pressure P = 0.5 Pa, deposition time t = 3 hours, b) t_d = 825 °C, deposition pressure P = 0.5 Pa, deposition time t = 3 hours. The nanoparticles for first sample shows particles stacked together. The mean size of these islands is d = 17.9 ± 1.5 nm. Second sample is composed of nanoparticles with mean size of d = 6.7 ± 1.1 nm in diameter.

particle includes ca. 2000 atoms, ~38% of them being at the surface. The surface changed from smoky black to colorless after taking the sample from the vacuum chamber. This indicates that the obtained Yb nanoparticles are easily oxidized. Figs.5 and 6 show the measured XRR (X-ray Reflectivity) curves for two different samples. It was found that the data can be interpreted well (R-factor less than 4%) when assuming two layers (combination of oxide and metallic layers or two oxide layers - due to the morphology of the sample) on the glass substrate, rather than using the single layer model. Fig.5 reveals that the top layer has a higher density than the second layer. Because of the density of Yb_2O_3 (9.17 g/cm^3) is quite higher than that of the Yb metal (6.90 g/cm^3) [1] and the density value of the model top layer is higher than that of the Yb metal, the top layer is interpreted as aYb_2O_3 and lower layer as aYb metal. The results give slightly

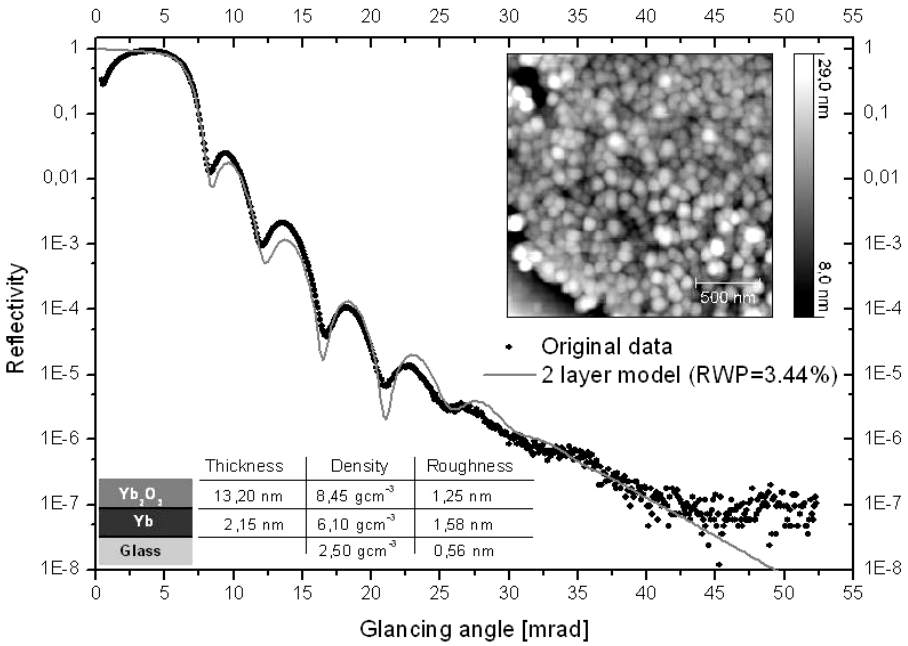

Fig.5 X-ray reflectivity for the sample prepared under the following conditions; deposition temperature t_d = 600°C, deposition pressure $P = 3.8 \times 10^{-6}$ Pa, deposition time t = 3 hours. The data are analyzed by the least-squares curve fitting with the 2-layer model. The obtained parameters are listed in a Table. The R_p ($= \Sigma|R_{exp}(i) - R_{calc}(i)| / \Sigma R_{exp}(i)$) and R_{wp} ($= (\Sigma w(i)(R_{exp}(i) - R_{calc}(i))^2 / \Sigma w(i) R_{exp}(i)^2))^{1/2}$ where $w(i) = 1$ in this case) in log scale were 3.06 % and 3.44%, respectively. The AFM image of a sample surface is shown in the inset.

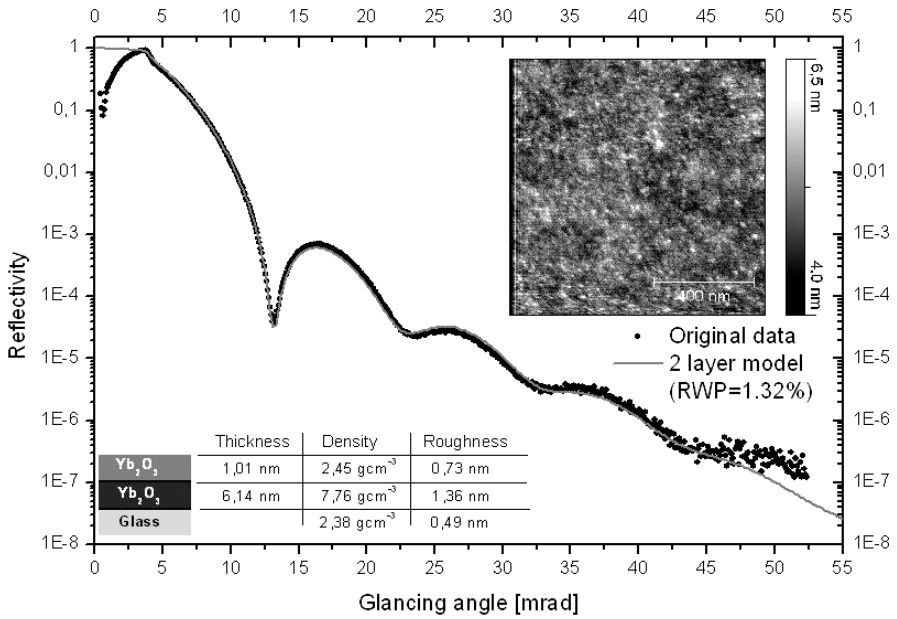

Fig.6 X-ray reflectivity for the sample prepared under the following conditions; deposition temperature t_d = 500°C, deposition pressure P = 3 Pa, deposition time t = 3 hours. The data are analyzed by the least-squares curve fitting with 2 oxide layers model. The obtained parameters are listed in a Table. The R_p and R_{wp} in log scale were 1.23 % and 1.32%, respectively. AFM image of sample surface is shown in the inset.

lower densities for both layers than those of bulk values. We think that this is mainly due to the growth mechanism (extremely soft landing on the substrate) and morphology of the particles.

Fig.6 shows the XRR data from another sample. The best model for this sample reveals again two layers but composed of oxide layers that differ mainly in electron density. The top layer has a much lower electron density than the lower layer. The density of the lower layer is 7.76 g/cm^3. This is a higher value than that of the Yb metal and reflects the sample morphology. The XRR measurement gives information only about the mean value parameters through the illuminated area. From the AFM images of this sample, one can see that the surface layer is composed of small nanoparticles with a mean diameter ~9.6 nm [7]. This surface layer of nanoparticles represents a thin low density layer obtained from the model. More heavy material is deposited under this layer.

From both examples, the XRR gives reliable information about the oxidation of Yb nanoparticles well. The sample is shown in Fig.7. The structure is not a single phase. In addition to a face-center cubic (fcc) Yb metal, some hexagonal Yb metal and oxides peaks were observed.

Another important parameter is roughness. We compared roughness obtained from XRR and AFM measurements. Both values differ randomly but not by more than three times. The difference could be due to non-uniformity of the samples, as AFM is a local measurement and XRR gives average values through the larger area. The typical and maximum

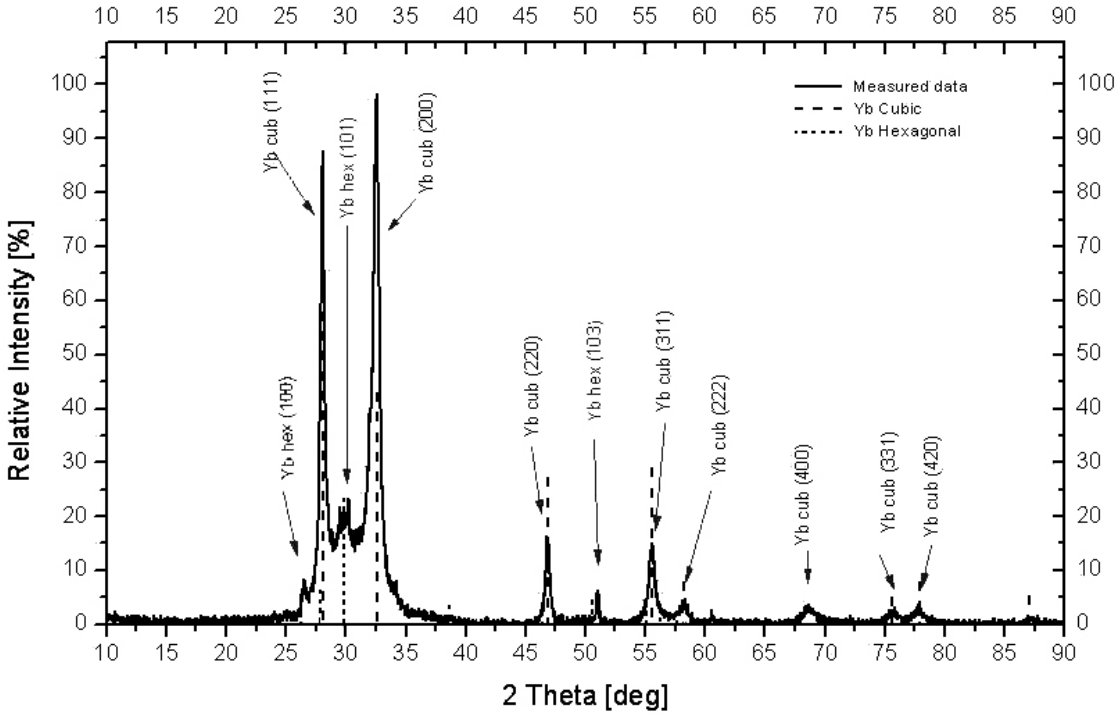

Fig.7 X-ray diffraction pattern measured for the sample prepared under the following conditions; deposition temperature t_d = 800°C, deposition pressure $P = 5 \cdot 10^{-5}$ Pa, deposition time t = 3 hours. The XRD pattern shows that the deposit is not single phase. The peaks from FCC and hexagonal ytterbium are observed..

Table 1 Nanopatricles equivalent diameter (in nm). Results have been obtained from the AFM image processing and the observed size was recalculated to the real nanoparticle size [7].

	0.5 Pa	3 Pa	10 Pa	25 Pa
500 °C	17. 9 ± 1.5	9.6 ± 2.2	—	—
600 °C	—	—	—	—
700 °C	—	1.6 ± 1.2	—	—
800 °C	4.5 ± 2.2	—	—	—
825 °C	6.7 ± 1.1	2.5 ± 1.8	3.7 ± 2.1	1.7 ± 1.2

Table 2 Thickness of deposited film (in nm) obtained from X-ray reflectivity curve modeling. The data are analyzed by the least-squares curve fitting using Parratt formula [6].

	Vacuum	0.5 Pa	3 Pa	10 Pa	25 Pa
500 °C	5.18	4.67	7.15	—	—
600 °C	15.37	5.12	—	—	—
700 °C	14.38	—	10.71	—	—
800 °C	34.70	12.66	4.50	—	—
825 °C	15.65	16.50	23.06	17.,40	4.77

observed roughnesses of the samples were around 1 nm and 5 nm, respectively. Table 1 shows the size of the Yb nanoparticles obtained at different evaporation temperatures and He pressures. The size of the nanoparticles was obtained by image processing of AFM images. The observed sizes were recalculated to their real values [7]. During the present experiments, it was not possible to find a clear dependence of the Yb particle size on the conditions, unlike with other metals. Some convection could make the system rather complicated, because of the quite low melting point of Yb. On the other hand, layer thickness has a simple clear dependence. Increasing the temperature and reducing the He partial pressure led to a higher deposition rate and higher layer thickness. The total layer thicknesses of the samples are shown in Table 2.

5. Conclusion

We succeeded in the preparation of Yb nanoparticles by the gas deposition method in a He atmosphere. The size, shape and morphology were studied by AFM and X-ray techniques. The studied particles have mainly a spherical shape and differ slightly in size for each sample. It was not possible to find a clear dependence of Yb particle size on deposition conditions [8]. Nevertheless, such dependence can be observed for layer thickness. Increasing the temperature and reducing the He partial pressure led to a higher deposition rate and in turn higher layer thickness.

The surface of Yb nanoparticles is oxidized as soon as being exposed to air. This can be observed visually by the change of the color of the deposit and confirmed

by XRR and XRD. The models of the deposits obtained by comparing measured XRR curves with calculated ones using the Parratt formula [6] consist typically of two layers where the top layer is composed of ytterbium oxide. Peaks from Yb_2O_3 can be observed in the XRD patterns. The XRD data revealed also that the nanoparticle thin film has no single phase. In addition to fcc an Yb metal, some hexagonal Yb metal peaks were observed.

The present study shows that it is possible to prepare ytterbium nanoparticles in a variety of sizes by employing the gas deposition method.

Acknowledgment

The work was done based on the collaboration program between the National Institute for Materials Science, Japan and Charles University, Czech Republic. The authors would like to thank Dr. M. Mizusawa for kind assistance during the research.

Reference

1) G.Hampel: " The Encyclopedia of Chemical Elements ", Reinhold Book Corporation, U.S.A. (1992).
2) J.A.Ascencio, A.C.Rodríguez-Monroy, H.B.Liu, G. Canizal: *Chem. Lett*., **33**, 1056 (2004).
3) C.G.Granqvist, R.A.Buhrman: *J. Appl. Phys*., **47**, 2200 (1976).
4) O.Starykov, K.Sakurai: *Appl. Surf. Sci*., **244**, 235 (2005); *Vacuum*, **80**, 117 (2005).
5) http://www.nims.go.jp/xray/lab/down/murex.htm; K. Sakurai, A.Iida: *Jpn. J. Appl. Phys*., **31,** L113 (1992); Adv. X-ray Anal., **35,** 813 (1992).
6) L.G.Parratt: *Phys. Rev*., **95**, 359 (1954).
7) C.Kacher, et al.: *Eur. Biophys. J*., **28**, 611 (2000).
8) M.Jerab, K.Sakurai: to be submitted to Journal of Physics: Condensed Matter.